A 9–31-GHz Subharmonic Passive Mixer in 90-nm CMOS Technology

Mingquan Bao, Harald Jacobsson, *Member, IEEE*, Lars Aspemyr, *Member, IEEE*, Geert Carchon, and Xiao Sun

***Abstract*—A subharmonic down-conversion passive mixer is designed and fabricated in a 90-nm CMOS technology. It utilizes a single active device and operates in the LO source-pumped mode, i.e., the LO signal is applied to the source and the RF signal to the gate. When driven by an LO signal whose frequency is only half of the fundamental mixer, the mixer exhibits a conversion loss as low as 8–11 dB over a wide RF frequency range of 9–31 GHz. This performance is superior to the mixer operating in the gate-pumped mode where the mixer shows a conversion loss of 12–15 dB over an RF frequency range of 6.5–20 GHz. Moreover, this mixer can also operate with an LO signal whose frequency is only 1/3 of the fundamental one, and achieves a conversion loss of 12–15 dB within an RF frequency range of 12–33 GHz. The IF signal is always extracted from the drain via a low-pass filter which supports an IF frequency range from DC to 2 GHz. These results, for the first time, demonstrate the feasibility of implementation of high-frequency wideband subharmonic passive mixers in a low-cost CMOS technology.**

***Index Terms*—90-nm CMOS, MMIC, passive mixer, subharmonic mixer, wideband.**

I. Introduction

In a transceiver system, the mixer is one of the key building blocks, converting signals from one frequency to another. Most mixers utilize the fundamental local oscillation (LO) signal to realize frequency conversion, but subharmonic mixers utilize second- or the third-order harmonics of the LO signal, generated by nonlinearities within the device. This allows the LO frequency of a subharmonic mixer to be one-half or even one-third of the LO frequency of a fundamental mixer. Therefore, a subharmonic mixer becomes attractive, especially in the millimeter-wave range where a low phase noise LO source is not readily available. Moreover, the subharmonic mixers mitigate LO self-mixing problems. LO self-mixing, caused by LO leakage to the RF port, creates a DC offset at the IF output, which is of particular importance for direct-conversion transceivers. To date, all published subharmonic mixers operating at high frequency are based on III–V technologies [1]–[8] with the SiGe mixer in [9] being the only exception. However, low-cost CMOS has potential to be an alternative technology to traditional III–V semiconductor technologies for implementing transceiver systems operating at microwave and millimeter-wave frequencies. A major reason for CMOS mixers not having been widely used is that RF performance of CMOS has not been good enough until recently. Except the mixer presented in [9], all reported subharmonic mixers in silicon are operated at low frequencies ($<$6 GHz) [10]–[13]. All of them are active mixers, which are one of the most power hungry circuits in a transceiver and often require a DC supply voltage above 1 V. Alternatively, passive mixers have become an attractive option for low DC power consumption and low supply voltage applications. Unfortunately, such mixers suffer from high conversion loss, typically larger than 10 dB when operating at one-half of the LO frequency of a fundamental mixer [1]–[6], and more than 20 dB when operating at one-third of the LO frequency [8]. Consequently, additional gain is required elsewhere in the receive (or transmit) chain offsetting the power consumption saved in the mixer itself. Therefore, reducing the conversion loss is a major design issue in passive subharmonic mixers. An approach to achieve low conversion loss is proposed here, that is to utilize an LO source-pumped mixer instead of the widely used LO gate-pumped mixer. In this paper, for the first time, a low conversion loss CMOS passive subharmonic mixer operating at frequencies up to 31 GHz is demonstrated. Furthermore, it is also shown that this CMOS mixer can operate with an LO signal whose frequency is not only one-half but also one-third of a fundamental mixer.

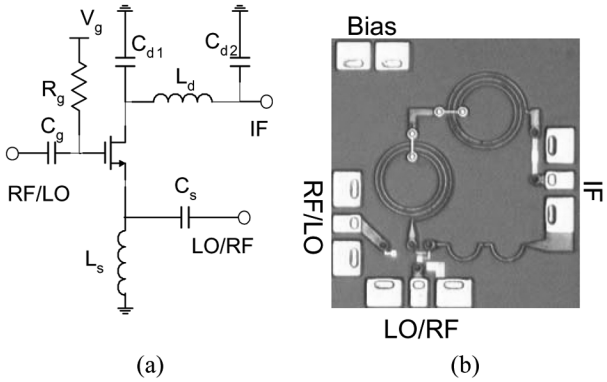

Fig. 1. (a) Schematic of subharmonic passive mixer. (b) Die photo of mixer with chip size of 0.9 mm × 1.0 mm.

II. Circuit Fundamentals

A. Circuit Topology

A schematic of the subharmonic passive mixer is shown in Fig. 1(a). The LO signal is applied to the source of the transistor and the RF signal to the gate, i.e., the mixer operates in a source-pumped mode. The IF signal is extracted from the drain via a low-pass filter. For comparison, this mixer can also work in gate-pumped mode, i.e., the LO signal applied to the gate of the transistor and the RF signal to the source.

Manuscript received November 30, 2005; revised April 6, 2006.

M. Bao, H. Jacobsson, and L. Aspemyr are with the Microwave and High Speed Electronics Research Center, Ericsson Research, Ericsson AB, Mölndal SE-43184, Sweden (e-mail: mingquan.bao@ericsson.com).

G. Carchon and X. Sun are with IMEC, Leuven B-3001, Belgium.

Digital Object Identifier 10.1109/JSSC.2006.881551

In the source node of the nMOS transistor, a series capacitor C_s and a shunt inductor L_s form a high-pass filter that suppresses unwanted IF signals and acts as an input matching network. The grounded terminal of L_s also sets the source DC voltage equal to zero. The gate bias is applied via a resistor R_g. An LO or RF signal is injected into the gate through a capacitor C_g, which is applied for DC decoupling and reducing the IF leakage to this port. At the drain, a π-network composed of C_{d1}, C_{d2}, and L_d acts as a low-pass filter. The total gate width and number of fingers of the nMOS transistor are selected carefully to minimize the conversion loss. Each gate finger is contacted from both sides to further reduce losses.

B. Circuit Analysis

When an LO signal is applied at the source, the gate-drain transconductance g_m varies. The time-dependent conductance, which contains fundamental and harmonic frequency components of the LO signal, will modify the RF signal applied to the transistor gate, and generates a drain current that contains different frequency components. Among them, a component at the IF frequency, $f_{\rm IF} = |f_{\rm RF} - nf_{\rm LO}|$, will be extracted by using a low-pass filter at the drain, where $n = 1, 2, \ldots$ is an integer. In the fundamental mixer, an IF signal corresponding to $n = 1$ is selected, whereas in the subharmonic mixer, an IF signal corresponding to $n > 1$ is utilized. Thus, in the subharmonic mixer, the LO frequency is only $1/n$ of that in the fundamental mixer, for the same RF and IF frequencies.

For an LO source-pumped subharmonic mixer, the amplitude of the desired IF signal is determined by the product of g_m and the RF signal at the gate. Therefore, the conversion efficiency depends on the variation of the gate-drain transconductance g_m, or more accurately, it depends on the amplitude of the second or the higher order harmonics of g_m. In contrast, the conversion efficiency of an LO gate-pumped mixer depends on the variation of the drain-source transconductance g_{ds}. It is well known that for a CMOS transistor the maximum value of g_m is larger than that of g_{ds}. Also, the variation of g_m is larger than that of g_{ds} because g_m and g_{ds} vary from their maximum value to zero when the transistor is switched between on and off by the LO signal. Therefore, it can be expected that a source-pumped mixer has less conversion loss than an LO gate-pumped mixer. This can also be verified by an analysis, based on a short-channel *I–V* CMOS model. The derivation procedure is the same as that for a subharmonic mixer in GaAs HEMT [7] except for the *I–V* model of the transistor. Details of the derivation are given in the Appendix. From the *I–V* model, we conclude that the drain current contains the wanted IF angular frequency $(\omega_{\rm RF} - 2\omega_{\rm LO})$. For the LO source-pumped mode, this component of the drain current is given by (A5):

$$I_{\rm D}(\omega_{\rm RF} - 2\omega_{\rm LO}) = K \cdot \left(\frac{1}{3\pi} + \frac{3\alpha}{32} V_{\rm LO}\right) V_{\rm LO} V_{\rm RF} \qquad (1)$$

and for the LO gate-pumped mode by (A9):

$$I_{\rm D}(\omega_{\rm RF} - 2\omega_{\rm LO}) = K \cdot \left(\frac{1}{3\pi} V_{\rm LO} V_{\rm RF}\right) \qquad (2)$$

where the parameters K and α are defined in the Appendix, and $V_{\rm LO}$ and $V_{\rm RF}$ are the voltage amplitudes of the LO and RF signals, respectively. Comparing (1) and (2), it can be found that the mixer operating in the LO source-pumped mode has a larger drain current at the desired IF frequency than the mixer operating in the LO gate-pumped mode, since the second term in (1) is always positive. Thus, we can draw the conclusion that for a given device and LO voltage swing, the LO source-pumped mixer has less conversion loss than the LO gate-pumped mixer.

The MOS Model 11 transistor model from Philips was used in simulations. EM simulations were carried out to extract model parameters for MIM capacitors, inductors, and transmission lines. While correlation between simulations and measurements was quite satisfactory for the mixer operating in the fundamental mode, the correlation in the subharmonic modes varied, being good under certain conditions and barely acceptable in others. It is not surprising that the subharmonic modes are difficult to reproduce in simulations since higher order effects determinate the behavior. However, to investigate precisely the reason for the discrepancies is beyond the scope of this paper.

C. Technology

The mixer described in this paper has been realized in a 90-nm CMOS technology [15]. Using an optimum transistor layout, the nMOS device has an $f_{\rm T}$ of 170 GHz and an $f_{\rm max}$ of 240 GHz. The process offers three back-end-of-line metal layers for interconnect, MIM capacitors and resistors. High Q-factor inductors are realized by an extra 5 μm thick, electroplated Cu layer on top of a 15 μm low-K dielectric BCB layer [14]. A die photo is shown in Fig. 1(b). The dimensions of the mixer chip are 0.94 mm $\times$ 1.0 mm including pads. The π-network occupies most of the die area, since it requires large inductance values in order to work well all the way down to DC.

III. Measured Performance

The mixer has been measured on-wafer in different subharmonic modes which include:

1) source-pumped LO signal whose frequency is 1/2 of that for the fundamental mixer;
2) source-pumped LO signal whose frequency is 1/3 of that for the fundamental mixer;
3) gate-pumped LO signal whose frequency is 1/2 of that for the fundamental mixer;
4) gate-pumped LO signal whose frequency is 1/3 of that for the fundamental mixer.

Since the measured conversion loss of the mixer operating in mode 4) is larger than 20 dB, the results of this mode will be omitted in the following. For briefness, we will in the following refer to the modes 1), 2) and 3) as "1/2-LO source-pumped", "1/3-LO source-pumped", and "1/2-LO gate-pumped", respectively.

A. Conversion Loss Measurements

One-tone measurements were carried out for different operational modes by using a spectrum analyzer. The losses of cables and probes were corrected in calibration. The cable losses versus frequencies were measured by using signal sources and power meters, while the probe losses were taken from data sheets. In

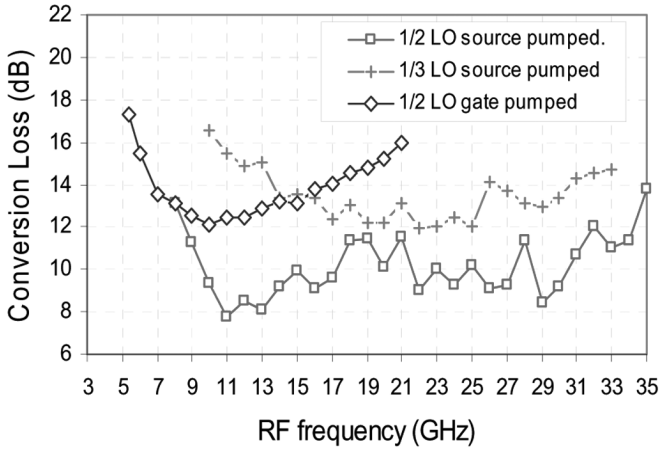

Fig. 2. Conversion loss of the subharmonic mixer versus RF frequency for a fixed IF frequency of 1 GHz.

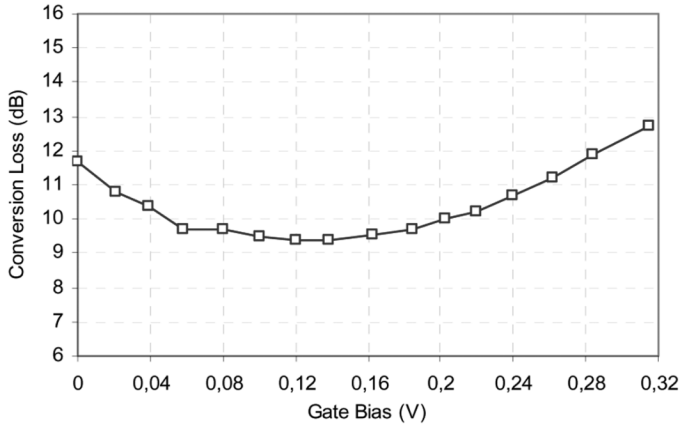

Fig. 3. Conversion loss of the mixer in the 1/2-LO source-pumped mode as a function of gate bias voltage, at an RF frequency of 30 GHz, an IF frequency of 1 GHz, an LO frequency of 14.5 GHz, and an LO power of 9.7 dBm.

Fig. 2, the conversion loss is plotted as a function of RF frequency for a fixed IF frequency of 1 GHz and at the optimum V_{gs} of the different modes, respectively. As shown in Fig. 2, the mixer in the 1/2-LO source-pumped mode has a conversion loss of 8–11 dB, which is lower than that of 12–15 dB in the 1/2-LO gate-pumped mode. Also, the 3-dB RF bandwidth in the 1/2-LO source-pumped mode is 9–31 GHz, which is much larger than the 6.5–20 GHz in the 1/2-LO gate-pumped mode.

Furthermore, we for the first time report a passive CMOS mixer operating in the 1/3-LO source-pumped mode. The conversion loss of the mixer in the 1/3-LO source-pumped mode is 12–15 dB within an RF frequency range of 12–33 GHz. This conversion loss is larger than in the 1/2–LO source-pumped modes because the amplitude of the third-order harmonic of the transconductance g_m is small.

The conversion loss of a subharmonic mixer is a function of the gate bias voltage. Because the gate bias voltage determines the duty cycle of the LO signal, consequently it determines the harmonics of the transconductance. In Fig. 3, the measured conversion loss versus gate bias is plotted for the mixer in the 1/2-LO source-pumped mode at an RF frequency of 30 GHz and an IF frequency of 1 GHz. This mixer is driven by an LO signal whose frequency and power are 14.5 GHz and 9.7 dBm, respectively. It can be seen that, as the gate bias increases from 0.05 V to 0.23 V, the variation of the conversion loss is less than 1 dB.

Meanwhile, for both the 1/2-LO gate-pumped and the 1/3-LO source-pumped mode, at $V_{gs} = 0$, the conversion loss has a minimum. The results plotted in Fig. 2 are measured at the optimal gate bias where the conversion loss is minimized.

The dependence of the conversion loss on the LO power is plotted in Fig. 4 for the three modes at an IF frequency of 1 GHz. For the 1/2-LO gate-pumped mode, the conversion loss shown in Fig. 4 is measured at an RF frequency of 14 GHz and an LO frequency of 6.5 GHz. As can be seen, an LO power of 3 dBm is sufficient in this mode. For the 1/2-LO source-pumped mode, the data shown in Fig. 4 is measured at an RF frequency of 30 GHz and an LO frequency of 14.5 GHz. The conversion loss in this mode saturates for LO powers larger than 10 dBm. Because the impedance at the source is smaller than that at the

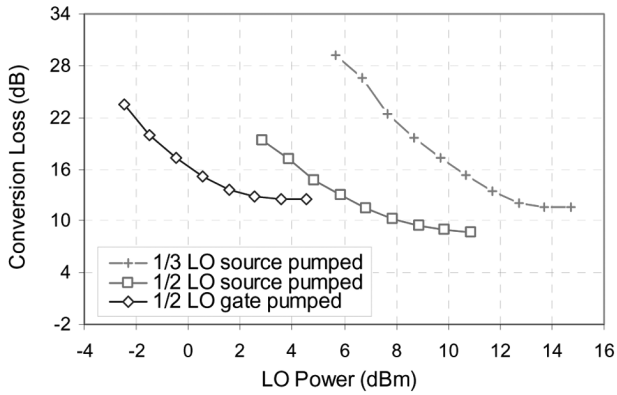

Fig. 4. Conversion loss of the subharmonic mixer versus LO power with a fixed IF frequency of 1 GHz. The LO frequency is 6.5, 6.33, and 14.5 GHz for the 1/2-LO gate-pumped mode, the 1/3-LO source-pumped mode, and the 1/2-LO source-pumped mode, respectively.

gate, a large LO input power is required in the source-pumped mode to obtain a comparable voltage swing. For the 1/3-LO source-pumped mode, the data is obtained at an RF frequency of 20 GHz and an LO frequency of 6.33 GHz. Here the conversion loss saturates for LO powers larger than 12.5 dBm. It is not surprising that the mixer in the 1/3-LO source-pumped mode requires the largest LO power to reach conversion loss saturation since the power level of the third-order harmonic of LO signal is always lower than the lower order harmonics. Even though the illustrated data were measured at different LO frequencies, the behavior of the conversion loss versus LO power is very similar at other LO frequencies.

It should be noted that the conversion loss plot in Fig. 2, is given for LO power levels where the conversion loss just reaches saturation for the different modes, in accordance with the data in Fig. 4. The LO power level was thus 3.3, 9.7, and 12.6 dBm for the 1/2-LO gate-pumped, the 1/2-LO source-pumped, and the 1/3-LO source-pumped modes, respectively.

The conversion loss varies with IF frequency in a quite similar way for the different modes. In Fig. 5, the measurement result for the 1/2-LO source-pumped mode is plotted for a fixed LO frequency of 14.5 GHz, an LO power of 9.7 dBm, and a gate bias of 0.12 V. The RF frequency varies between 29.05 GHz

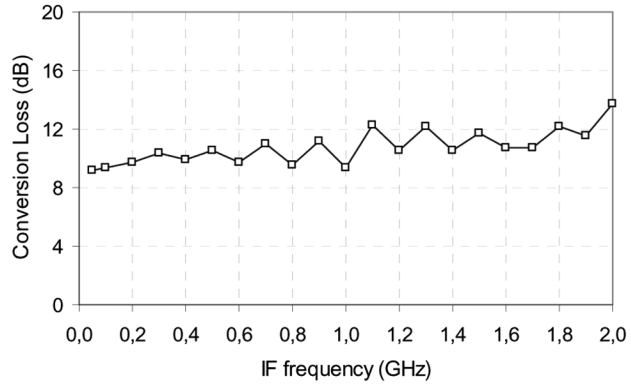

Fig. 5. Conversion loss of the 1/2-LO source-pumped mode mixer versus IF frequency at LO frequency of 14.5 GHz, LO power of 9.7 dBm, and a gate bias of 0.12 V. The RF frequency varies from 29.05 to 31 GHz.

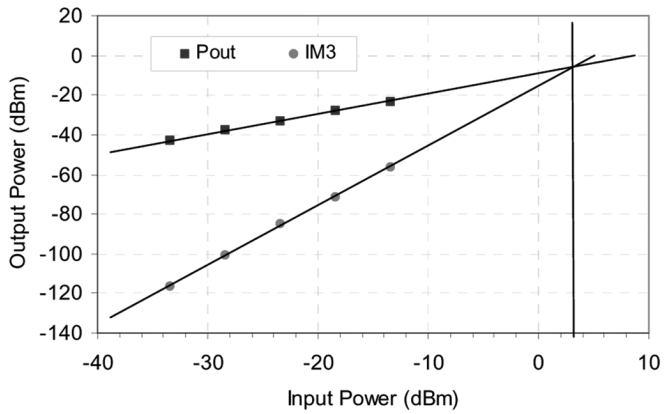

Fig. 6. For the 1/2-LO source-pumped mode, the fundamental and third-order intermodulation IF components versus RF input power, at RF frequency of 20 GHz, LO frequency of 9.5 GHz, and IF frequency of 1 GHz, LO power of 9.7 dBm.

TABLE I
SUMMARY OF MINIMUM ISOLATION BETWEEN PORTS FOR THE DIFFERENT SUBHARMONIC MODES

	1/2-LO-gate-pumped	1/2-LO-source-pumped	1/3-LO-source-pumped
LO-to-IF (dB)	37.7	22.5	28.6
LO-to-RF (dB)	19	17	21.7
2LO-to-IF (dB)	—	55.7	47.6
2LO-to-RF (dB)	27.2	27	29.4
3LO-to-IF (dB)	—	—	67.2
3LO-to-RF (dB)	—	—	45.7
RF-to-IF (dB)	22.5	37.7	37.7

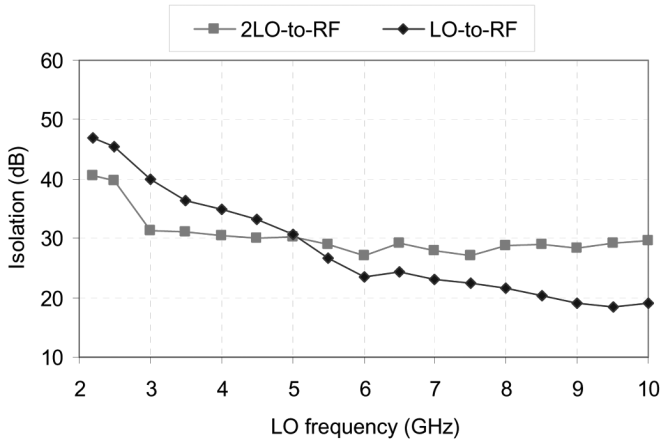

Fig. 7. For the 1/2-LO gate-pumped mode, the isolation of LO signal and its higher order components to the RF port.

and 31 GHz, corresponding to an IF frequency varying between 50 MHz and 2 GHz. Fig. 5 shows that the 3-dB IF bandwidth of the mixer is around 1.8 GHz. An important property of the mixer is that it works very well down to low IF frequencies. In fact, the design of the IF filter is made with a direct conversion architecture in mind and the results indeed confirm that the mixer could work well all the way down to zero IF.

B. IIP3 Measurements

The third-order intermodulation intercept point (IIP3) performance of the mixer is determined by two-tone measurements. Fig. 6 shows the measured results for the mixer operating in the 1/2-LO source-pumped, where the RF and IF frequencies are 20 GHz and 1 GHz, respectively. As can be seen the IIP3 of the 1/2-LO source-pumped mode is 3 dBm. Measured under similar conditions, the IIP3 of the mixer in the 1/3-LO source-pumped mode is found to be 7 dBm. The higher IIP3 for the 1/3-LO source-pumped mode comes at the cost of a higher conversion loss.

The measured IIP3 for the 1/2-LO gate-pumped mode is 7 dBm both at an RF frequency of 10 and 14 GHz. Taking the varying conversion loss of the different mixer modes into account by comparing the output referred IP3, the results show that the mixer in the 1/2-LO source-pumped mode and the 1/2-LO gate-pumped mode has a similar linearity. However, the linearity of this subharmonic passive mixer is not as good as that of a similar fundamental passive mixer [18], [19].

C. Isolation Between Ports

In Table I, the measured minimum port-to-port isolation is summarized for the three subharmonic modes, where the isolation of 2Port_1-to-Port_2 or 3Port_1-to-Port_2 represents the ratio between input power at Port_1 and the second-order or the third-order harmonic measured at Port_2. In the 1/2-LO gate-pumped mode, both the LO-to-RF and 2LO-to-RF isolation are plotted in Fig. 7. It can be found that the 2LO-to-RF isolation is around 30 dB when LO frequencies vary from 3 to 10 GHz. In the 1/2-LO source-pumped configuration, both the LO-to-IF and the 2·LO-to-IF isolation exceed 22 dB over an LO frequency range from 4 to 17 GHz. Meanwhile, the minimum LO-to-RF and 2·LO-to-RF isolation is 17 and 27 dB, respectively, within the same LO frequency range, as shown in Fig. 8. However, the latter is more important for the 1/2-LO source-pumped or the 1/2-LO gate-pumped mode. The reason is that it is difficult to filter out the second harmonic of the LO signal at the RF port because $2f_{\text{LO}}$ and f_{RF} are too close in frequency. Similarly, the 3LO-to-RF isolation, as shown in Fig. 9, which is larger than 45 dB, is important for the 1/3-LO source-pumped mixer. Due

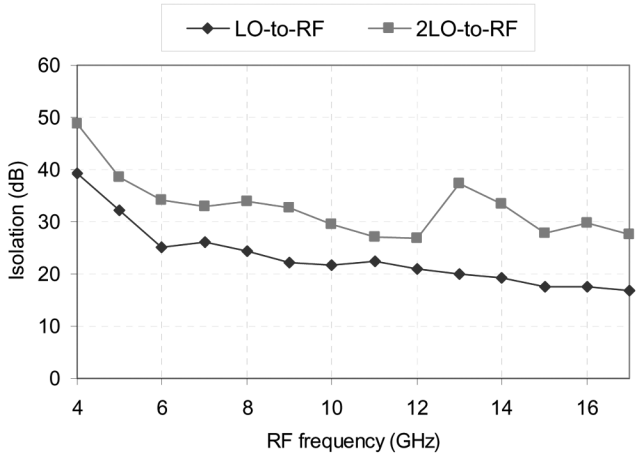

Fig. 8. For the 1/2-LO source-pumped mode, the isolation of the LO signal and its second-order components to the RF port.

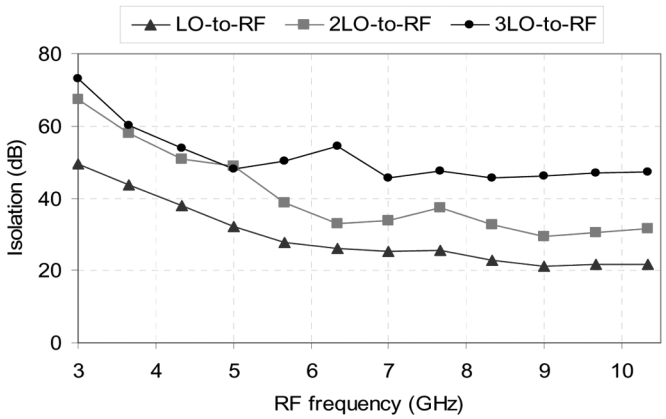

Fig. 9. For the 1/3-LO source-pumped mode, the isolation of the LO signal and its higher order components to the RF port.

to the low-pass filter at the IF port, the RF-to-IF isolation is quite good.

The S11 data measured at the gate and the source ports are plotted in Fig. 10. In the source-pumped mode, S11, measured at the gate port, decreases from -3.6 to -7.5 dB within the RF frequency range of 9–31 GHz. In the gate-pumped mode, S11, measured at the source port, is much lower, less than -8 dB over most of the frequency range of 6.5–20 GHz.

Since a CMOS mixer in a real application will most likely be integrated with a low-noise amplifier (LNA), it is not at all obvious that 50 Ω is the optimum impedance level. Therefore, the data given in Fig. 10 should be used for a better understanding of the frequency behavior of the mixer. The actual impedance level and matching may then be traded for other parameters.

IV. Comparison With Reported Mixers

In Table II, a comparison between this work and previously reported 1/2-LO gate-pumped and 1/3-LO gate-pumped subharmonic mixers is presented. It can be seen that the mixer in this work, operating in the 1/2-LO source-pumped mode achieves the widest bandwidth, 22 GHz, among the reported subharmonic mixers. Together with the low conversion loss, the

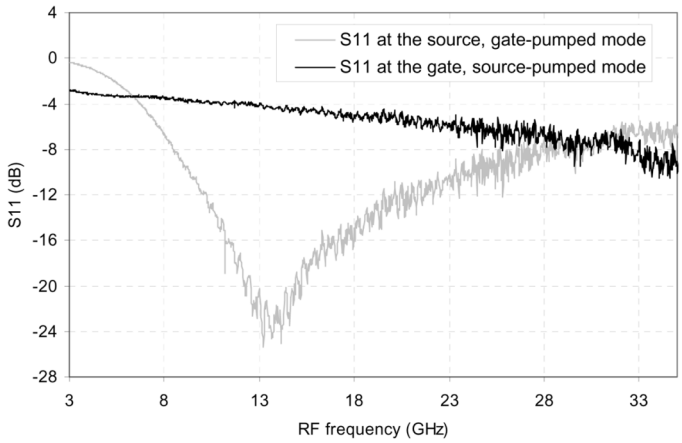

Fig. 10. The S11 data measured at the gate and source ports, for the mixer in the source-pumped mode and in the gate-pumped mode, respectively.

wide bandwidth makes this subharmonic mixer very competitive in comparison to previously reported passive subharmonic mixers based on III–V semiconductor technologies. When the mixer presented here is operating in the 1/3-LO source-pumped mode, the minimum conversion loss of 12 dB is 8 dB better than that of the AlInAs–GaInAs mixer of the same type [8].

V. Conclusion

A single-ended subharmonic passive mixer based on a 90-nm CMOS technology has been investigated. It exhibits a low conversion loss and wide RF frequency bandwidth, both for the 1/2-LO and the 1/3-LO frequency modes, as well as a decent port-to-port isolation. However, the linearity of this mixer is not as good as a fundamental passive mixer. The analysis and measurements results indicate that the source-pumped mode is superior to the gate-pumped mode in terms of conversion gain. The results presented illustrate that 90-nm CMOS subharmonic passive mixers, using a topology well suited for an MMIC implementation, are capable of achieving very good performance at frequencies up to the millimeter-wave region.

Appendix

In this Appendix, expressions for the subharmonic components of the drain current are derived for LO source-pumped and LO gate-pumped mixers. For the sake of simplicity, the expressions in the following are derived under the condition that the gate bias voltage V_g is equal to the threshold voltage $V_{\rm T}$. Thus, the device is only on during half of the LO signal cycle. Furthermore, the parasitic effects are not taken into account. The following analysis is used only to make a qualitative comparison between the LO source-pumped and gate-pumped modes. It is not accurate enough to determine conversion losses.

I. LO Source-Pumped Mode

In the LO source-pumped mode, the RF signal is applied at the gate and the LO signal at the source. During the positive excursions of the LO signal, the device is shut down, but during negative excursions, the transistor could operate in the saturation region, even though no DC supply voltage is applied at the drain, since both the gate-source voltage $V_{\rm GS}$ and the

TABLE II
COMPARISON OF REPORTED SUBHARMONIC MIXERS

Technology		RF (GHz)	Con. Gain (dB)	LO power (dB)	Chip size (mm^2)	Ref.
0.2μm GaAs PHEMT*		10-12	-6.5	12	—	[1]
0.15μm GaAs PHEMT*		40-45	-10	7	—	[2]
0.25μm GaAs PHEMT*		32-40	-13 – -17	4-5	2.31	[3]
0.25μm GaAs PHEMT*		30-40	-14 – -22	13	3	[4]
0.15μm GaAs PHEMT*		75-88	-14 – -18	5	1.5	[5]
0.15μm GaAs PHEMT*		27.5-28.5	-11	13	2	[6]
0.15μm GaAs PHEMT***		85-92	-4.7 – -10	11	2	[7]
AlInAs-GaInAs HFET**		50-60	-21.5	7	—	[8]
SiGe***		75-86	0.7 – 2.5	10	0.77	[9]
90nm CMOS	1/2 LO Source pumped	9-31	-8 – -11	9.7	1	This work
	1/2 LO Gate pumped	6.5-20	-12 – -15	3.3	1	
	1/3 LO Source pumped	12-33	-12 – -15	12.6	1	

*1/2-LO-gate-pumped; **1/3-LO-gate-pumped, *** 1/2-LO-gate-pumped and active mixers.

drain-source voltage $V_{\rm DS}$ increases. The device delivers current only in the lower half-cycle of the LO signal. In this case, the LO voltage can be represented by its negative half-cycle period through a Fourier series [7]

$$f(\omega_{\rm LO}t) = V_{\rm LO}\left[\frac{1}{\pi} - \frac{1}{2}\sin(\omega_{\rm LO}t) - \frac{2}{\pi}\left(\frac{\cos(2\omega_{\rm LO}t)}{1\cdot 3} + \frac{\cos(4\omega_{\rm LO}t)}{3\cdot 5} + \frac{\cos(6\omega_{\rm LO}t)}{5\cdot 7} + \cdots\right)\right] \quad \text{(A1)}$$

where $V_{\rm LO}$ is the amplitude of the LO signal. The amplitude of the drain current at the IF frequency $I_D(\omega_{\rm RF} - 2\omega_{\rm LO})$ is derived based on a short-channel *I–V* CMOS model. In the saturation region ($V_{\rm DS} > V_{\rm DSat}$), the drain current $I_{\rm D}$ can be expressed as [16]

$$\begin{aligned} I_{\rm D} &= \frac{K}{2}\cdot\frac{(V_{\rm GS}-V_{\rm T})^2}{1+\alpha(V_{\rm GS}-V_{\rm T})} \\ &\approx \frac{K}{2}\cdot(V_{\rm GS}-V_{\rm T})^2 \\ &\quad\times\left[1-\alpha(V_{\rm GS}-V_{\rm T})+\alpha^2(V_{\rm GS}-V_{\rm T})^2-\cdots\right] \\ &= \frac{K}{2}\cdot\left[(V_{\rm GS}-V_{\rm T})^2\right. \\ &\qquad\left.-\alpha(V_{\rm GS}-V_{\rm T})^3+\alpha^2(V_{\rm GS}-V_{\rm T})^4-\cdots\right] \end{aligned} \quad \text{(A2)}$$

where the parameter K is determined by the technology and the size of the device, and α approximately models the combined mobility degradation (represented by θ) and effects of velocity saturation $v_{\rm sat}$, and α is given by

$$\alpha = \theta + \frac{\mu_0}{2v_{\rm sat}L} \quad \text{(A3)}$$

where μ_0 is the mobility of the charge carriers, L is gate length and θ is a fitting parameter. θ is approximately given by $\theta = (2\times 10^{-9})/t_{\rm ox}$ [17], where $t_{\rm ox}$ is the thickness of the oxide under the gate. The value of the parameter α increases with downscaling of the CMOS devices [16].

The term $(V_{\rm GS} - V_{\rm T})$ in (A2) is given by

$$\begin{aligned} V_{\rm GS}-V_{\rm T} &= V_{\rm RF}\sin(\omega_{\rm RF}t) - f(\omega_{\rm LO}t) + V_g - V_{\rm T} \\ &= V_{\rm RF}\sin(\omega_{\rm RF}t) - f(\omega_{\rm LO}t) \end{aligned} \quad \text{(A4)}$$

where $V_{\rm RF}$ is the amplitude of the RF signal. Inserting (A4) into (A2), it can be found that the first and the second terms in (A2) contain the IF angular frequency [7]:

$$I_{\rm D}(\omega_{\rm RF} - 2\omega_{\rm LO}) = K\cdot\left(\frac{1}{3\pi} + \frac{3\alpha}{32}V_{\rm LO}\right)V_{\rm LO}V_{\rm RF}. \quad \text{(A5)}$$

II. LO GATE-PUMPED MODE

In the LO gate-pumped mode, the RF signal is applied at the source and the LO signal at the gate. If it is assumed that no LO/RF signals nor their harmonics appear at the drain, since they are grounded via capacitor C_{d1}, the drain-source voltage is mainly determined by the RF signal:

$$V_{\rm DS} = -V_{\rm RF}\sin(\omega_{\rm RF}t). \quad \text{(A6)}$$

The applied RF signal at the source is not large enough to drive the transistor into the saturation operating region. Thus, the CMOS operates only in the triode region ($V_{\rm DS} < V_{\rm DSat}$) and the drain current $I_{\rm D}$ is given by

$$\begin{aligned} I_{\rm D} &= K\cdot\frac{(V_{\rm GS}-V_{\rm T}-\frac{1}{2}V_{\rm DS})\cdot V_{\rm DS}}{1+\alpha V_{\rm DS}} \\ &\approx K\cdot\left[(V_{\rm GS}-V_{\rm T})-\frac{1}{2}V_{\rm DS}\right] \\ &\quad\times\left(V_{\rm DS}-\alpha V_{\rm DS}^2+\alpha^2V_{\rm DS}^3-\cdots\right). \end{aligned} \quad \text{(A7)}$$

The device conducts current only during the higher half-cycle of the LO signal:

$$\begin{aligned} V_{\rm GS} - V_{\rm T} &= f(\omega_{\rm LO}t - \pi) - V_{\rm RF}\sin(\omega_{\rm RF}t) + V_g - V_{\rm T} \\ &= f(\omega_{\rm LO}t - \pi) - V_{\rm RF}\sin(\omega_{\rm RF}t). \end{aligned} \tag{A8}$$

Therefore, from (A6)–(A8) we know that only the term $(V_{\rm GS} - V_{\rm T})\,V_{\rm DS}$ contains a component at the IF angular frequency $(\omega_{\rm RF} - 2\omega_{\rm LO})$ given by

$$I_{\rm D}(\omega_{\rm RF} - 2\omega_{\rm LO}) = K \cdot \left(\frac{1}{3\pi}V_{\rm LO}V_{\rm RF}\right). \tag{A9}$$

Finally, it should be pointed out that, in the case of $V_g \neq V_{\rm T}$, the Fourier expansion of the periodical LO voltage (A1) will be different, but the derivation procedure as mentioned above can still be used.

ACKNOWLEDGMENT

The authors would like to thank Dr. T. Lewin and Prof. H. Zirath for helpful discussions and encouragement.

REFERENCES

[1] H. Zirath, "A subharmonically pumped resistive dual-HEMT-mixer," in *IEEE MTT-S Int. Microwave Symp. Dig.*, 1991, pp. 875–878.

[2] H. Zirath, I. Angelov, and N. Rorsman, "A millimeterwave subharmonically pumped resistive mixer based on a heterostructure field effect transistor technology," in *IEEE MTT-S Int. Microwave Symp. Dig.*, 1992, pp. 599–602.

[3] K. S. Ang, A. H. Baree, S. Nam, and I. D. Robertson, "A millimeterwave monolithic subharmonically pumped resistive mixer," in *Proc. Asia Pacific Microwave Conf.*, 1999, pp. 222–225.

[4] K. S. Ang, M. Chongcheawchamman, D. Kpogla, P. R. Young, I. D. Robertson, D. S. Kim, M. C. Ju, and H. C. Seo, "Monolithic Ka-band even-harmonic quadrature resistive mixer for direct conversion receivers," in *IEEE Radio Frequency Integrated Circuits (RFIC) Symp. Dig. Papers*, 2001, pp. 169–172.

[5] M. F. Lei, P. S. Wu, T. W. Huang, and H. Wang, "Design and analysis of miniature W-band MMIC subharmonically pumped resistive mixer," in *IEEE MTT-S Int. Microwave Symp. Dig.*, 2004, pp. 235–238.

[6] P. C. Yeh, W. C. Liu, and H. K. Chiou, "Compact 28-GHz subharmonically pumped resistive mixer MMIC using a lumped-element high-pass/band-pass balun," *IEEE Trans. Microw. Wireless Compon. Lett.*, vol. 15, no. 2, pp. 62–64, Feb. 2005.

[7] Y. J. Hwang, H. Wang, and T. H. Chu, "A W-band subharmonically pumped monolithic GaAs-based HEMT gate mixer," *IEEE Trans. Microw. Wireless Compon. Lett.*, vol. 14, no. 7, pp. 313–315, Jul. 2004.

[8] H. Zirath, I. Angelov, N. Rorsman, C. Kalsson, and M. Sironen, "A millimeter-wave AlInAs-GaInAs HFET-based subharmonically pumped mixer," in *Proc. Eur. Microwave Conf.*, 1995, pp. 294–298.

[9] J. J. Hung, T. M. Hancock, and G. M. Rebeiz, " A 77 GHz SiGe subharmonic balanced mixer," *IEEE J. Solid-State Circuits*, vol. 40, no. 11, pp. 2167–2173, Nov. 2005.

[10] L. Sheng, J. C. Jensen, and L. E. Larson, "A wide-bandwidth Si/SiGe HBT direct conversion sub-harmonic mixer/downconverter," *IEEE J. Solid-State Circuits*, vol. 35, no. 9, pp. 1329–1337, Sep. 2000.

[11] M. Goldfarb, E. Balboni, and J. Gavey, "Even harmonic double-balanced active mixer for use in direct conversion receivers," *IEEE J. Solid-State Circuits*, vol. 38, no. 10, pp. 1762–1766, Oct. 2003.

[12] R. Svitek and S. Raman, "5–6 GHz SiGe active I/Q subharmonic mixer with power supply noise effect characterization," *IEEE Trans. Microw. Wireless Compon. Lett.*, vol. 14, no. 7, pp. 319–321, Jul. 2004.

[13] K. J. Jon, M. Y. Park, C. S. Kim, and H. K. Yu, " Subharmonically pumped CMOS frequency conversion (up and down) circuits for 2-GHz WCDMA direct-conversion transceiver," *IEEE J. Solid-State Circuits*, vol. 39, no. 6, pp. 871–884, Jun. 2004.

[14] G. J. Carchon, X. Sun, G. Posada, D. Linten, and E. Beyne, "Thin-film as enabling passive integration technology for RF SoC and SiP," in *IEEE Int. Solid-State Circuits Conf. (ISSCC) Dig. Tech. Papers*, 2005, pp. 398–399.

[15] W. Jeamsaksiri, D. Linten, S. Thijs, G. Carchon, J. Ramos, A. Mercha, X. Sun, P. Soussan, M. Dehan, T. Chiarella, R. Venegas, V. Subramanian, A. Scholten, P. Wambacq, R. Velghe, G. Mannaert, N. Heylen, R. Verbeeck, W. Boullart, I. Heyvaert, M. I. Natarajan, G. Groeseneken, I. Debusschere, S. Biesemans, and S. Decoutere, "A low-cost 90nm RF CMOS platform for record RF circuit performance," in *Symp. VLSI Technology Dig. Tech. Papers*, 2005, pp. 60–61.

[16] M. T. Terrovitis and R. G. Meyer, "Intermodulation distortion in current-commutating CMOS mixers," *IEEE J. Solid-State Circuits*, vol. 35, no. 10, pp. 1461–1473, Oct. 2000.

[17] T. H. Lee, *The Design of CMOS Radio-Frequency Integrated Circuits*. Cambridge, U.K.: Cambridge Univ. Press, 1998.

[18] F. Ellinger, "26.5-30-GHz resistive mixer in 90-nm VLSI SOI CMOS technology with high linearity for WLAN," *IEEE Trans. Microw. Theory Tech.*, vol. 53, no. 8, pp. 2559–2565, Aug. 2005.

[19] M. Bao, H. Jacobsson, L. Aspemyr, A. Mercha, and G. Carchon, "A 20 GHz sub-1V low noise amplifier and a resistive mixer in 90 nm CMOS technology," in *Proc. Asia-Pacific Microwave Conf.*, 2005, vol. 5.

Mingquan Bao received the B.S. and M.S. degrees in electrical engineering from Zhejiang University, Hangzhou, China, in 1985 and 1988, respectively, and the Ph.D. degree in radar remote sensing from the University of Hamburg, Hamburg, Germany, in 1995.

From 1995 to 1997, he was with the Institute of Oceanography, University of Hamburg. From 1997 to 2000, he was with the Center for Remote Imaging Sensing and Processing, University of Singapore, Singapore. From 2000 to 2001, he was with the German Aerospace Center (DLR), Germany. His research focus was on interferometric radar remote sensing. Since 2001, he has been with the Microwave and High-Speed Electronics Research Center, Ericsson AB, Sweden. His research interests include the RFIC designs such as low-noise amplifiers, mixers, and oscillators in the silicon and GaAs technologies.

Harald Jacobsson (M'00) received the M.S. degree in engineering physics and the Ph.D. degree in physics from Chalmers University of Technology, Gothenburg, Sweden, in 1986 and 1993, respectively.

From 1994 to 1996, he worked with the epitaxy and characterization of SiGe and SiGeC films at Arizona State University. Between 1996 and 2005, he was working at the Microwave and High Speed Electronics Research Center at Ericsson AB with the design of Si-based integrated circuits for microwave radio applications. Since 2006, he has been Manager of the MMIC and RFIC design group within the Microwave link organization at Ericsson.

Lars Aspemyr (M'05) received the M.Sc. degree in electrical engineering from Chalmers University, Gothenburg, Sweden, in 1992. He is currently working towards the Ph.D. degree in the Department of Electroscience, Lund University, Sweden.

He is also employed at Ericsson AB, Gothenburg, Sweden. His current research interest is in low-power high-frequency integrated circuit design.

Geert Carchon received the M.Sc. and Ph.D. degrees in electronic engineering from the K.U. Leuven, Leuven, Belgium, in 1996 and 2001, respectively, where he worked on the measurement, modeling and design of monolithic and thin-film microwave integrated circuits.

In 2001, he joined the Interuniversity MicroElectronics Centre (IMEC), Leuven, Belgium, where he is currently heading the Microwave and RF System-in-Package team. His research interests include RF and millimeter-wave thin-film integrated passives and modules, RF MEMS, GaN power amplifiers, above-IC technology, and mm-wave CMOS design. In these fields, he has authored or co-authored over 100 papers for international conferences and journals and written two book chapters.

Dr. Carchon received the Outstanding Paper Award at IMAPS2003.

Xiao Sun received the M.S. degree from Institute National Polytechnique of Grenoble (INPG), France, in 1998, and the Ph.D. degree from the University of Joseph Fourier, France in 2001, both in electrical engineering.

Since 2002, she has been a Research Engineer in the Design for Analog and RF Technologies and Systems group, Interuniversity MicroElectronics Centre (IMEC), Belgium. Her main research interests include electromagnetic simulation, RF systems and multichip modules. Her present focus is on integrated passive components and interconnects for above-IC functions.